

# X-Ray Magnetic Circular Dichroism Picks out Single-Molecule Magnets Suitable for Nanodevices

By Matteo Mannini, Francesco Pineider, Philippe Sainctavit, Loïc Joly, Arantxa Fraile-Rodríguez, Marie-Anne Arrio, Christophe Cartier dit Moulin, Wolfgang Wernsdorfer, Andrea Cornia, Dante Gatteschi, and Roberta Sessoli\*

The encoding of magnetic information at the molecular level finds in Single Molecule Magnets (SMM) a most promising avenue.<sup>[1]</sup> SMM are composed of discrete metal-ion clusters which assemble into molecular crystals and offer unparalleled chemical flexibility and processability among soft magnetic materials. Their ground state has a large spin value and an easy-axis magnetic anisotropy, so that at low temperature the reversal of the molecular magnetic moment is subject to an energy barrier which can be overcome either via thermal activation or by a quantum-tunneling mechanism.<sup>[1]</sup> Each molecule in the crystal thus behaves as a nanometer-sized magnet, displaying hysteresis<sup>[2]</sup> and fascinating quantum effects.<sup>[3,4]</sup> Applications of SMM in ultrahigh-density information storage and spintronics are foreseen,<sup>[5]</sup> which entail SMM organized into addressable layers at surfaces<sup>[6–8]</sup> or incorporated into metal-molecule-metal junctions.<sup>[9–11]</sup> However, fundamental aspects related to the magnetic behavior of SMM in these environments have not yet been fully explored. In fact, the spin dynamics of SMM is exceedingly sensitive to structural deformations, intermolecular interactions, and to other environmental effects, which are expected to be different for SMM hosted in a crystalline lattice, assembled into an addressable layer or incorporated in a metal-molecule-metal

junction. Recently we have reported a magneto-optical investigation on the archetypal SMM, the mixed-valence Mn<sub>12</sub> complex, in different environments showing the disappearance of magnetic hysteresis when the clusters are organized as a SAM on gold.<sup>[12]</sup> Further studies are necessary to assess if the slow magnetization dynamics that characterizes SMM behavior is compatible with the surface environment. With this goal in mind we have used X-ray magnetic circular dichroism, XMCD,<sup>[13,14]</sup> at sub-Kelvin temperatures to investigate the surface magnetic properties of thin films made of two different SMM. We show here that SMM behavior is indeed observable for the first monolayer(s) but, surprisingly, not in the case of the widely investigated Mn<sub>12</sub> clusters.

The object systems of this study are [Mn<sub>12</sub>O<sub>12</sub>(O<sub>2</sub>CR)<sub>16</sub>(H<sub>2</sub>O)<sub>4</sub>], Mn<sub>12</sub>,<sup>[1,15]</sup> and [Fe<sub>4</sub>(L)<sub>2</sub>(dpm)<sub>6</sub>], Fe<sub>4</sub>,<sup>[16,17]</sup> where Hdpm is dipivaloylmethane and H<sub>3</sub>L is a tripodal ligand derived from 2-hydroxymethyl-1,3-propanediol. Both types of clusters are characterized by a large spin value of the ground state,  $S = 10$  and  $S = 5$ , respectively, and an easy-axis magnetic anisotropy which generates an energy barrier for magnetization reversal of approximately 70 and 20 K, respectively. Chemical modification of these systems is relatively easy to achieve and a large variety of products with different terminal groups have been prepared. Some of them are able to bind to substrates like metallic or semiconductor surfaces (both pristine and pre-functionalized),<sup>[6]</sup> or can be integrated in a molecular electronics device.<sup>[10,11]</sup> The derivatives employed in this study, whose structures are shown in Figure 1a and b, have RCO<sub>2</sub>H = 4-(methylthio)benzoic acid<sup>[15]</sup> and H<sub>3</sub>L = 11-(acetylthio)-2,2-bis(hydroxymethyl)undecan-1-ol, respectively.<sup>[17]</sup>

Samples were prepared by drop-casting millimolar solutions of each SMM in dichloromethane on a clean and flat polycrystalline Au(111) support and allowing for complete solvent evaporation. All operations were carried out in a portable glove box directly connected to the preparation chamber of the XMCD setup (see Experimental Section). Films with thickness of a few hundred nanometers were employed here for two reasons: i) the role of the substrate, including its possible redox activity,<sup>[7]</sup> is negligible when we monitor the topmost layers of the deposit through XMCD; ii) the magnetism of the entire thickness of the film can be investigated by standard magnetometry techniques and, by comparison, the effects of the unusual environment that characterizes the first molecular layers can be evidenced.

We carried out a bulk magnetic characterization on Mn<sub>12</sub> and Fe<sub>4</sub> samples using a vibrating sample magnetometer (vsm) and a micrometric superconducting quantum interference device ( $\mu$ -SQUID), respectively. The results are reported in Figure 1. A

[\*] Prof. R. Sessoli, Dr. M. Mannini, F. Pineider, Prof. D. Gatteschi  
Department of Chemistry and INSTM research unit, University of  
Florence

V. della Lastruccia 3, 50019, Sesto Fiorentino (FI) (Italy)  
E-mail: roberta.sessoli@unifi.it

Prof. P. Sainctavit, Dr. M. Arrio  
Institut de Minéralogie et de Physique des Milieux Condensés,  
UMR7590

Université Pierre et Marie Curie, Case 115  
4 place Jussieu, 75252 Paris Cedex 5 (France)

Dr. L. Joly, Dr. A. Fraile-Rodríguez  
Swiss Light Source, Paul Scherrer Institut, Villigen PSI  
5232 Villigen (Switzerland)

Dr. C. Cartier dit Moulin  
Laboratoire de Chimie Inorganique et Matériaux Moléculaires  
Université Pierre et Marie Curie  
Case 42, 4, place Jussieu 75252 Paris Cedex 5 (France)

Dr. W. Wernsdorfer  
Institut Néel, CNRS & Université Joseph Fourier, BP 166  
25 Avenue des Martyrs, 38042 Grenoble Cedex 9 (France)

Prof. A. Cornia  
Department of Chemistry and INSTM Research Unit, University of  
Modena and Reggio Emilia  
Via G. Campi 183, 41100, Modena (Italy)

DOI: 10.1002/adma.200801883

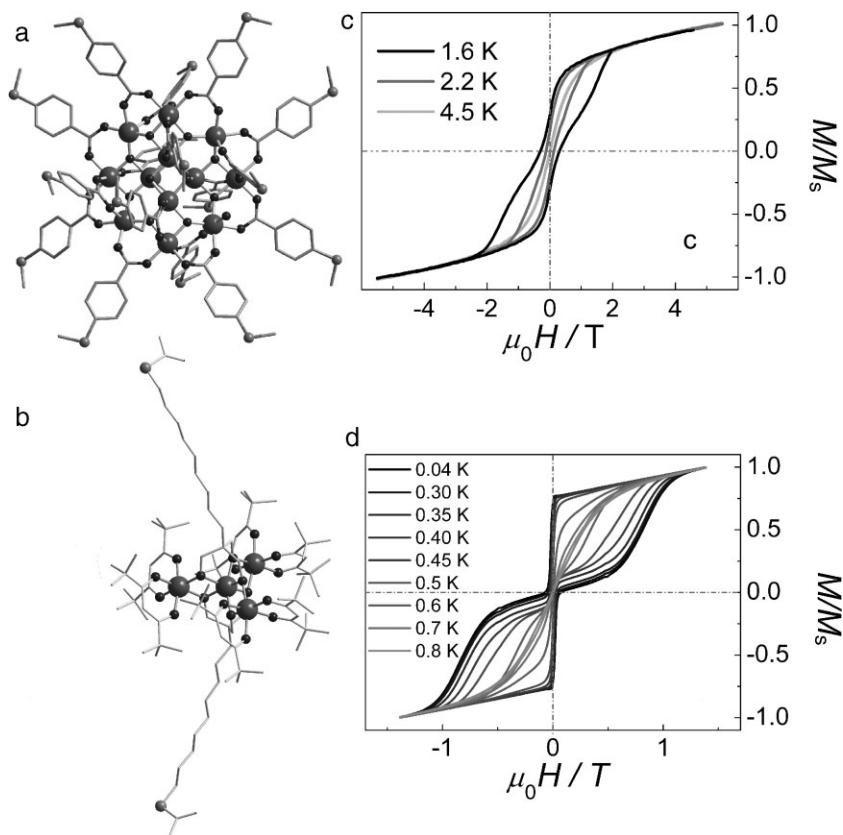


**Figure 1.** a) and b) Molecular structure of  $Mn_{12}$  and  $Fe_4$  clusters, respectively, with metal ions depicted as large dark gray spheres, oxygen as small dark gray spheres, sulphur as middle gray spheres and carbon as pale gray rods. c) and d) Magnetic hystereses of the entire thickness of thin films of  $Mn_{12}$  and  $Fe_4$  recorded using a vsm and a  $\mu$ -SQUID setup, respectively, at different temperatures with a sweeping rate of  $2 \text{ mT s}^{-1}$ .

temperature-dependent hysteresis loop is observed below 3 K in  $Mn_{12}$  but only below 1 K in  $Fe_4$ , in accordance with the lower anisotropy barrier of the latter. Moreover, the hysteresis has a different shape in the two compounds. In  $Fe_4$  quantum tunneling is more efficient than in  $Mn_{12}$ , especially close to zero field, thus giving rise to a rapid decrease of the magnetization and to a butterfly-shaped hysteresis loop.

X-ray absorption spectra (XAS) at the  $Mn-L_{2,3}$  and  $Fe-L_{2,3}$  edges have been recorded using left and right circularly polarized light at the Swiss Light Source (SLS), which exhibited optimal X-ray beam stability. The surface sensitivity of the Total Electron Yield (TEY) detection mode<sup>[18,19]</sup> was exploited to probe the first layer(s) of the two films. The XMCD spectra were obtained as the difference between the XAS spectra recorded for antiparallel ( $\sigma_-$ ) and parallel ( $\sigma_+$ ) alignment of the photon helicity with respect to the applied magnetic field.<sup>[20,21]</sup> Measurements were performed with the magnetic field and the photon beam normal to the film. Sub-Kelvin temperatures were reached by employing a specially designed  $^3\text{He}$ - $^4\text{He}$  dilution refrigerator setup.<sup>[22]</sup>

In Figure 2a we report the XAS spectra of  $Mn_{12}$  at the  $Mn-L_{2,3}$  edges and the associated XMCD signal. The observed spectral features are identical to those of the archetypal  $Mn_{12}$ -acetate derivative, and are indicative of antiferromagnetic interactions between  $Mn^{III}$  and  $Mn^{IV}$  spins in the core, as depicted in the inset

of Figure 2.<sup>[7,23]</sup> No modification of the spectra, including the uprising of features attributable to  $Mn^{II}$ , were observed during the entire exposure to the X-ray flux, confirming that photo-reduction is not occurring under the optimized conditions of our set-up. By measuring the field dependence of the intensity of the XMCD signal at the highest XMCD positive peak of the  $L_3$ -edge we have recorded element-specific hysteresis loops (Fig. 2b). Even if a field sweeping-rate similar to that used in Figure 1c is employed no opening of the hysteresis loop is observed down to the lowest investigated temperature,  $T = 0.75(5) \text{ K}$ . As the TEY detection mode probes only the first nanometers of the deposit, we argue that the first layers of molecules show drastically different magnetization dynamics. X-ray fluorescence, probing a thicker part of the sample, would have provided an interesting comparison; however, the low temperature set-up is incompatible with the fluorescence detection mode.

The XAS spectrum of  $Fe_4$  at the  $Fe-L_{2,3}$  edges is shown in Figure 3, along with the corresponding dichroic signal. As the XAS/XMCD response of this class of SMM has not been reported earlier, an extensive analysis based on a Ligand Field Multiplets model<sup>[20,24]</sup> has been carried out (see Experimental Section for more details). While the XAS spectra indicate that only  $Fe^{III}$  is present and no radiation damage occurs, the simulation of the XMCD data has confirmed the ferrimagnetic spin structure of the cluster with the central spin antiferromagnetically coupled to the three external ones (see inset of Fig. 4).<sup>[16,17]</sup> This allows us to conclude that the topmost layers comprise intact clusters.

In order to investigate the field dependence of the magnetization, the photon energy corresponding to the strongest negative XMCD peak at  $L_3$ -edge was selected and the results are shown in Figure 4. As expected, the hysteresis loop at  $1.4(2) \text{ K}$  is closed. When lowering the temperature below 1 K an irreversibility becomes visible and a significant hysteresis is observed at  $T = 0.55(5) \text{ K}$  (Fig. 4). The butterfly shape of the hysteresis and its temperature dependence strongly resemble those detected by traditional magnetometry (Fig. 1d), thus confirming that the SMM behavior is retained also in the first layers of clusters. It is worth to point out that the observation of hysteresis is a nice indirect proof that samples can be cooled down to sub-Kelvin temperatures in an UHV environment under prolonged exposure to an intense X-ray flux.

To get some insight in the anomalous behavior of  $Mn_{12}$  we compared field-dependent XMCD data to the predicted bulk magnetization at the same temperature as a function of applied field. The magnetization was evaluated using the energy levels calculated from the simple Spin Hamiltonian:

$$\mathcal{H} = D\hat{S}_z^2 + g\mu_B\mathbf{H} \cdot \mathbf{S} \quad (1)$$

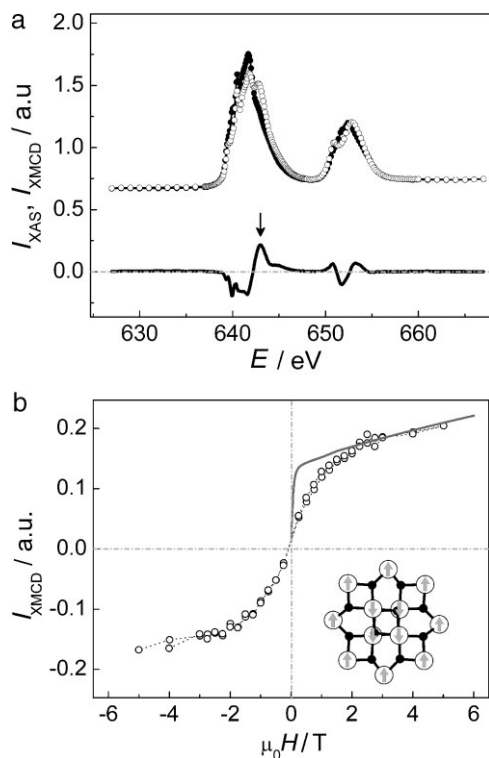


**Figure 2.** XAS and XMCD analysis on Mn<sub>12</sub>. a) Absorption spectra (○ = σ<sub>-</sub>; ● = σ<sub>+</sub>) and dichroic signal (black solid line) at T = 0.75 K and M<sub>OH</sub> = 3.0 T. b) Magnetic field dependence (○) of the XMCD signal at 643.0 eV, highlighted by the arrow in (a), compared to the expected magnetization curve for a bulk powder-like sample (gray solid line). A sweeping rate of 2 mT s<sup>-1</sup> has been employed. In the inset the magnetic core of Mn<sub>12</sub> and its ferrimagnetic spin structure.

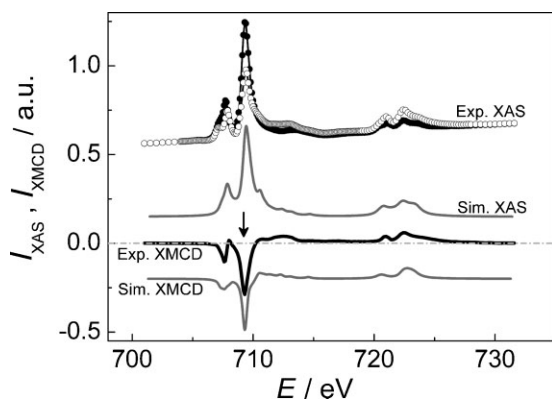


**Figure 3.** XAS and XMCD analysis on Fe<sub>4</sub>. Absorption spectra (○ = σ<sub>-</sub>; ● = σ<sub>+</sub>) and dichroic signal (black solid line) at T = 0.75 K and μ<sub>OH</sub> = 3.0 T, along with simulated curves (gray solid lines) obtained using Ligand Field Multiplet calculations. The arrow indicates the energy used to measure the field dependence and the simulated absorption spectrum corresponds to (σ<sub>-</sub> + σ<sub>+</sub>)/2.

where **H** is the magnetic field, *g* the Landé factor, μ<sub>B</sub> the Bohr magneton, and *D* < 0 describes the easy-axis magnetic anisotropy. The magnetization was averaged over all possible field orientations, as appropriate for randomly-oriented clusters at the

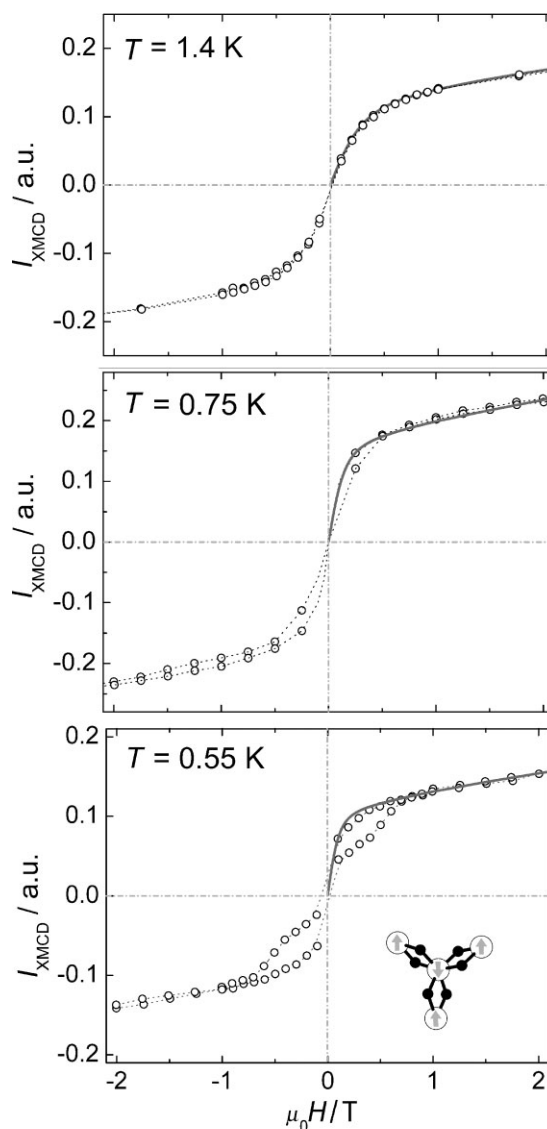


**Figure 4.** Magnetic field dependence of the XMCD signal of Fe<sub>4</sub> at 709.2 eV (multiplied by -1) for three different temperatures (open circles). Each curve is compared to the expected magnetization curve for a bulk powder-like sample (gray solid line). A sweeping rate of 2 mT s<sup>-1</sup> has been employed. In the inset the magnetic core of Fe<sub>4</sub> and its ferrimagnetic spin structure.

surface. A very good agreement is observed for Fe<sub>4</sub>, as shown in Figure 4, assuming the same Spin-Hamiltonian parameters determined on bulk samples, i.e., *S* = 5, *D*/*k<sub>B</sub>* = -0.629 K, and *g* = 2.00.<sup>[17]</sup> If the same procedure is repeated for Mn<sub>12</sub> with *S* = 10, *D*/*k<sub>B</sub>* = -0.66 K and *g* = 2.00,<sup>[1]</sup> the calculated field dependence is found to deviate significantly from the corresponding dichroic signal (Fig. 2b). In particular, the latter increases less abruptly at low field, suggesting that the molecules in the first layers experience a reduced anisotropy, even if no changes in the oxidation states are detected by the XAS investigation.

Given the extreme conditions of the XMCD experiments, we have developed an alternative experiment to confirm the unexpected difference in the dynamic behavior of Fe<sub>4</sub> and Mn<sub>12</sub>. Since the hysteresis of SMM has a dynamic origin,<sup>[2]</sup> the remnant magnetization undergoes in first approximation an exponential decay whose characteristic time,  $\tau$ , increases on lowering the temperature. To avoid the fast tunneling of the magnetization,<sup>[3,4]</sup> and the lower signal-to-background ratio of the TEY mode when operated in zero field, we first magnetized the samples in a +2.0 T magnetic field and then rapidly changed the field setting to -0.25 T. As soon as the target field was reached, the XMCD signal was measured as a function of time. The results for Fe<sub>4</sub>, obtained at 709.2 eV, are shown in Figure 5a. The dichroic signal has been found to vary in time and the data could be satisfactorily reproduced with a single exponential decay. To the best of our knowledge this is the first report of the measurement of the decay of the magnetization in real time using XMCD. The above described procedure described in the following has revealed to be particularly efficient for the magnetic characterization of nanostructured SMM and its introduction in characterization protocols is foreseen, even if it requires very good photon flux stability.

The measurement was carried out at two different temperatures and the characteristic time was found to increase on lowering the temperature, going from  $\tau = 87(5)$  s at  $T = 0.75(5)$  K to  $\tau = 285(10)$  s at  $T = 0.55(5)$  K. In Figure 5c these two data are included in an Arrhenius plot ( $\ln(\tau)$  vs.  $1/T$ ) evaluated on a similar sample using  $\mu$ -SQUID magnetometer. The magnetization dynamics at the surface of Fe<sub>4</sub> thin-film deposits and in bulk samples are thus comparable. By contrast, the dichroic signal of Mn<sub>12</sub> at 643.0 eV exhibits no significant time dependence (see Fig. 5b), therefore confirming that the magnetization relaxes much faster in the first monolayers of Mn<sub>12</sub>, despite the large hysteresis detected when investigating the entire thickness of the film.

These results demonstrate that the magnetic hysteresis of molecular origin that characterizes SMM is compatible with the very atypical environment found at the surface interphase, though

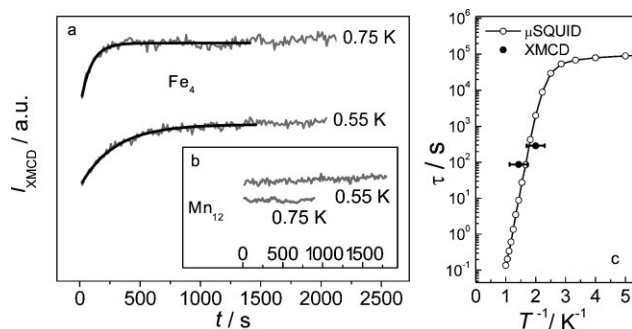


**Figure 5.** Time dependence of the dichroic signals. The samples are magnetized in a strong positive magnetic field (+2.0 T), then the field is rapidly ramped to a moderate negative value (-0.25 T) and the time dependence of the dichroic signal is measured. a) Time dependent signal observed for Fe<sub>4</sub> (gray solid lines), simulated with a mono-exponential decay (black solid lines). b) Time independent signal observed for Mn<sub>12</sub>. c) Relaxation times extracted from the XMCD signal decay (●) superimposed to the Arrhenius plot (-○-) obtained by investigating the whole thickness of the Fe<sub>4</sub> sample with a  $\mu$ -SQUID magnetometer.

a careful choice of the material is crucial. In particular the magnetism of Mn<sub>12</sub>-type complexes appears to be very sensitive to the environment and SMM behavior is completely lost at the surface of bulk samples. Since XAS measurements allow to rule out alterations in metal oxidation states as well as in the spin structure, structural deformations are probably responsible for the absence of hysteresis. Mn<sub>12</sub> derivatives are indeed known to give raise to Jahn–Teller isomerism,<sup>[25]</sup> whereupon the Jahn–Teller elongation axis of a Mn<sup>III</sup> ion is directed perpendicular rather than parallel to the molecular axis, resulting in a reduced anisotropy barrier. By contrast, in Fe<sub>4</sub> the tripodal ligands lying above and below the plane of the iron atoms are likely to impose a more rigid structure.<sup>[16]</sup>

In conclusion, by using XMCD at sub-Kelvin temperatures we have unambiguously shown here that SMM behavior of Fe<sub>4</sub> clusters is compatible with the surface environment. Despite the low blocking temperature this rich family of clusters is attracting increasing interest. In fact, the recent observation of a long decoherence time suggests that spin manipulation in quantum computing is feasible on these high spin clusters.<sup>[26]</sup> We can now envisage the next challenging step toward the realization of single-molecule devices able to exploit the peculiar magnetic behavior of SMM. It is in fact necessary to confirm that the magnetic hysteresis is retained when SMM are grafted on conducting surfaces. The sub-Kelvin XMCD setup used in this work, combined with the high beam stability of SLS, are expected to provide the required sensitivity.

## Experimental

Mn<sub>12</sub>O<sub>12</sub>(O<sub>2</sub>CR)<sub>16</sub>(H<sub>2</sub>O)<sub>4</sub> [RCO<sub>2</sub>H = 4-(methylthio)benzoic acid] and [Fe<sub>4</sub>(L)<sub>2</sub>(dpm)<sub>6</sub>] (H<sub>3</sub>L = 11-(acetylthio)-2,2-bis(hydroxymethyl) undecan-1-ol; Hdpm = dipivaloylmethane) were synthesized following reported preparation methods [15,17]. Pure, crystalline samples were dissolved in dichloromethane (99.8% purity, purchased from Fluka) to give  $\sim 10^{-3}$  M solutions. Au(111)-mica substrates (Agilent inc.) were treated with a hydrogen flame and immersed in EtOH in order to allow proper surface cleaning and reconstruction prior to deposition. Samples were prepared by dropping  $\sim 50 \mu\text{L}$  of the solutions on the freshly-annealed gold substrates and allowing for complete solvent evaporation. All operations were carried out in a portable glove box directly connected to the preparation chamber of the XMCD setup.

The TBT XMCD setup used in these experiments has been described elsewhere [22]. Briefly, it consists of a <sup>3</sup>He–<sup>4</sup>He dilution refrigerator especially designed to reach temperatures of the order of (500 ± 5) mK in an UHV environment. The magnetic field has been applied with superconducting Helmholtz coils along the direction of the X-rays with a maximum amplitude of (7 ± 0.001) T; this end-station has been connected to the SIM beamline at the Swiss Light Source, Paul Scherrer Institut, Switzerland [27].

XAS spectra were recorded in TEY mode [18,19] with an energy resolution better than 100 meV. The beamline optics was tuned to reduce the photon flux density at the sample to avoid the effect of radiation damage, as already done in previous investigations [7]. In order to minimize systematic errors, the XMCD spectrum was obtained by recording XAS with all possible combinations of field polarity and light circular polarization. The hysteresis curves were recorded by monitoring the field dependence of the dichroic signal at the energy of its maximum. Though SLS light stability was crucial for the success of the experiments, we found that a further improvement of the signal could be achieved by switching the polarization continuously before each variation of the field. The magnetic measurements on the Mn<sub>12</sub> film were carried out using a

vibrating sample magnetometer (Oxford Instruments MAGLAB2000), while for the bulk characterization of Fe<sub>4</sub> film we exploited the low temperature capabilities of the  $\mu$ -SQUID setup described in ref. [28].

The  $L_{2,3}$  edges spectra were calculated by using the Ligand Field Multiplet code developed by Thole [24] in the framework established by Cowan [29] and Butler [30]. This approach takes into account all of the electronic Coulombic repulsions, the 3d and 2p spin-orbit coupling, and treats the geometrical environment of the absorbing atom by a crystal field potential [31]. The spectrum is calculated as the sum of all possible transitions for an electron jumping from the 2p to the 3d level in the electric dipole approximation. The electric dipole allowed 2p to 4s transitions are neglected. The interelectronic repulsions are introduced through Slater integrals calculated by an atomic Hartree-Fock model. For the simulation of the Fe<sup>III</sup>  $L_{2,3}$  edges in Fe<sub>4</sub>, the Slater integrals were scaled by a reduction factor  $\kappa = 60\%$  to account for the electronic delocalization. The surrounding of the Fe<sup>III</sup> ions was described by an octahedral crystal field with  $10 Dq = 1.5$  eV.

## Acknowledgements

A large part of this work was performed at the Swiss Light Source, Paul Scherrer Institut, Villigen, Switzerland. We acknowledge Fabrice Scheurer, Jean-Paul Kappler and Bernard Müller from the IPCMS for their help in equipment installation, and the staff of the SIM beamline for their support. This research project was supported by the EU, within the EU FP6, through the Key Action: Strengthening the European Research Area, Research Infrastructures, Contract no.RI13-CT-2004-506008, through NoE MAGMANet (NMP3-CT-2005-515767) and through the ERANET project "NanoSci-ERA: NanoScience in the European Research Area". It was also partially funded by CNR through Comma PM.P05.011 and by Italian MIUR through FIRB (RBNE033KMA) and PRIN projects.

Received: July 4, 2008

Published online: October 23, 2008

- [1] D. Gatteschi, R. Sessoli, J. Villain, *Molecular Nanomagnets*, Oxford University Press, Oxford **2006**.
- [2] R. Sessoli, D. Gatteschi, A. Caneschi, M. A. Novak, *Nature* **1993**, 365, 141.
- [3] J. R. Friedman, M. P. Sarachik, J. Tejada, R. Ziolo, *Phys. Rev. Lett.* **1996**, 76, 3830.
- [4] L. Thomas, F. Lioni, R. Ballou, D. Gatteschi, R. Sessoli, B. Barbara, *Nature* **1996**, 383, 145.
- [5] L. Bogani, W. Wernsdorfer, *Nat. Mater.* **2008**, 7, 179.
- [6] A. Cornia, A. C. Fabretti, L. Zoppi, A. Caneschi, D. Gatteschi, M. Mannini, R. Sessoli, *Single-Molecule Magnets and Related Phenomena*, Structure & Bonding Book Series, Vol.122, Springer, Berlin **2006**, pp133.
- [7] M. Mannini, P. Sainctavit, R. Sessoli, C. Cartier dit Moulin, F. Pineider, M.-A. Arrio, A. Cornia, D. Gatteschi, *Chem. Eur. J.* **2008**, 14, 7530.
- [8] S. Voss, M. Fonin, U. Rüdiger, M. Burgert, U. Groth, Y. S. Dedkov, *Phys. Rev. B* **2007**, 75, 045102.
- [9] G. H. Kim, T. S. Kim, *Phys. Rev. Lett.* **2004**, 92, 137203.
- [10] H. B. Heersche, Z. de Groot, J. A. Folk, H. S. J. van der Zant, C. Romeike, M. R. Wegewijs, L. Zoppi, D. Barreca, E. Tondello, A. Cornia, *Phys. Rev. Lett.* **2006**, 96, 206801.
- [11] M.-H. Jo, J. E. Grose, K. Baheti, M. Deshmukh, J. J. Sokol, E. M. Rumberger, D. N. Hendrickson, J. R. Long, H. Park, D. C. Ralph, *Nano Lett.* **2006**, 6, 2014.
- [12] L. Bogani, L. Cavigli, M. Gurioli, R. L. Novak, M. Mannini, A. Caneschi, F. Pineider, R. Sessoli, M. Clemente-León, E. Coronado, A. Cornia, D. Gatteschi, *Adv. Mater.* **2007**, 19, 3906.
- [13] P. Gambardella, A. Dallmeyer, K. Maiti, M. C. Malagoli, W. Eberhardt, K. Kern, C. Carbone, *Nature* **2001**, 416, 301.
- [14] H. Wende, M. Bernien, J. Luo, C. Sorg, N. Pompadian, J. Kurde, J. Miguel, M. Piantek, X. Xu, P. Eckhold, W. Kuch, K. Baberschke, P. M. Panchmatia, B. Sanyal, P. M. Oppeneer, O. Eriksson, *Nat. Mater.* **2007**, 6, 516.
- [15] L. Zoppi, M. Mannini, M. Pacchioni, G. Chastanet, D. Bonacchi, C. Zanardi, R. Biagi, U. Del Pennino, D. Gatteschi, A. Cornia, R. Sessoli, *Chem. Commun.* **2005**, 1640.
- [16] S. Accorsi, A.-L. Barra, A. Caneschi, G. Chastanet, A. Cornia, A. C. Fabretti, D. Gatteschi, C. Mortalò, E. Olivieri, F. Parenti, P. Rosa, R. Sessoli, L. Sorace, W. Wernsdorfer, L. Zoppi, *J. Am. Chem. Soc.* **2006**, 128, 4742.
- [17] A.-L. Barra, F. Bianchi, A. Caneschi, A. Cornia, D. Gatteschi, L. Gorini, L. Gregoli, M. Maffini, F. Parenti, R. Sessoli, L. Sorace, A. M. Talarico, *Eur. J. Inorg. Chem.* **2007**, 4145.
- [18] R. Nakajima, J. Stöhr, Y. U. Idzerda, *Phys. Rev. B* **1999**, 59, 6421.
- [19] Y. Ufuktepe, G. Akgül, J. Lüning, *J. Alloys Compd.* **2005**, 401, 193.
- [20] F. M. F. de Groot, A. Kotani, *Core Level Spectroscopy of Solids*, Advances in Condensed Matter Science, Vol. 6, CRC Press, Boca Raton, U.S.A., **2008**.
- [21] J. Stöhr, *J. Magn. Magn. Mater.* **1999**, 200, 470.
- [22] I. Letard, P. Sainctavit, C. Cartier dit Moulin, J.-P. Kappler, P. Ghigna, D. Gatteschi, B. Doddi, *J. Appl. Phys.* **2007**, 101, 113920-1-6.
- [23] R. Moroni, C. Cartier dit Moulin, G. Champion, M.-A. Arrio, P. Sainctavit, M. Verdaguer, D. Gatteschi, *Phys. Rev. B* **2003**, 68, 064407.
- [24] B.-T. Thole, G. van der Laan, J. C. Fuggle, G. A. Sawatzky, R. C. Karnatak, J.-M. Esteve, *Phys. Rev. B* **1985**, 32, 5107.
- [25] S. M. J. Aubin, Z. Sun, H. J. Eppley, E. M. Rumberger, I. A. Guzei, K. Folting, P. K. Gantzel, A. L. Rheingold, G. Christou, D. N. Hendrickson, *Inorg. Chem.* **2001**, 40, 2127.
- [26] C. Schlegel, J. van Slageren, M. Manoli, E. K. Brechin, M. Dressel, *Phys. Rev. Lett.* **2008**, in press. Preprint available at <http://arxiv.org/abs/0807.0303>.
- [27] C. Quitmann, U. Flechsig, L. Patthey, T. Schmidt, G. Ingold, M. Howells, M. Janousch, R. Abela, *Surf. Sci.* **2001**, 480, 173.
- [28] W. Wernsdorfer, K. Hasselbach, A. Benoit, W. Wernsdorfer, B. Barbara, D. Mailly, J. Tuaillon, J. P. Perez, V. Dupuis, J. P. Dupin, G. Guiraud, A. Perex, *J. Appl. Phys.* **1995**, 78, 7192.
- [29] R. D. Cowan, *The Theory of Atomic Structure and Spectra*, University of California Press, Berkeley **1981**.
- [30] P. H. Butler, *Point Group Symmetry, Applications, Methods and Tables*, Plenum, New York **1991**.
- [31] F. M. F. de Groot, J. C. Fuggle, B. T. Thole, G. A. Sawatzky, *Phys. Rev. B* **1990**, 42, 5459.